Chapter 8
Symmetry-Directed Design of Protein Cages and Protein Lattices and Their Applications

Aaron Sciore and E. Neil G. Marsh

Abstract The assembly of individual protein subunits into large-scale structures is important in many biological contexts. Proteins may assemble into geometrical cages or extended lattices that are characterized by a high degree of symmetry; examples include viral capsids and bacterial S-layers. The precisely defined higher order structure exhibited by these assemblies has inspired efforts to design such structures *de novo* by applying the principles of symmetry evident in natural protein assemblies. Here we discuss progress towards this goal and also examples of natural protein cages and lattices that have been engineered to repurpose them towards a diverse range of applications in materials science and nano-medicine.

Keywords Protein assembly • Protein cages • Protein lattices • Computational protein design • Symmetry • Synthetic biology • Biomaterials • Nanomedicine

8.1 Introduction

In recent years our understanding of protein-protein interactions has blossomed, driven by advances in techniques such as native mass spectrometry, x-ray crystallography, electron microscopy, and computational modeling. The assembly of proteins into highly ordered, large-scale oligomeric structures has been found to play an important role in an increasing number of biological phenomena. At the same time our understanding of the principles by which proteins oligomerize has advanced to the point that it is now possible to rationally design such structures (Jha et al. 2010; Huang et al. 2007). This is an exciting development, as it paves the way for the design of protein-based nanomaterials that assemble in a highly ordered manner.

A. Sciore
Department of Chemistry, University of Michigan, Ann Arbor, MI 48109, USA
e-mail: sciore@umich.edu

E.N.G. Marsh (✉)
Department of Chemistry, University of Michigan, Ann Arbor, MI 48109, USA

Department of Biological Chemistry, University of Michigan, Ann Arbor, MI 48109, USA
e-mail: nmarsh@umich.edu

J.R. Harris, J. Marles-Wright (eds.), *Macromolecular Protein Complexes*,
Subcellular Biochemistry 83, DOI 10.1007/978-3-319-46503-6_8

Such materials are very attractive for industrial and medicinal applications as they are biocompatible, retain their biological function and may exhibit new properties that emerge as a consequence of their higher order structure.

This chapter is focused on applying the principles of symmetry, exhibited in naturally occurring protein assemblies, to the design of new protein-based nanomaterials. Initially, we briefly review some examples of naturally formed symmetric protein assemblies, primarily to illustrate how their oligomeric structures relate to their biological functions. Next we discuss various approaches that have been taken to repurpose protein assemblies for therapeutic and materials science applications. In the last part of the chapter we will describe the basic theory underlying approaches to designing symmetrical protein assemblies, followed by a fairly comprehensive survey of the methods that have been used to create *de novo* designed protein assemblies.

8.2 Natural Protein Assemblies

The self-association of protein subunits is a ubiquitous feature of biology. It is essential to functions as diverse as catalysis and regulation of enzymes, cell signaling, cytoskeleton maintenance and cell motility, sequestering of metabolic pathways, iron storage and packaging of nucleic acids by viruses. Proteins generally self-associate through complementary and highly specific hydrophobic interfaces on their surfaces. Except for the case of a symmetrical dimer, each protein subunit will have two (or more) self-association interfaces. The precise orientation of these interfaces relative to each other defines whether the protein will self-assemble into either an extended structure, represented by one-dimensional fibers and two- and three-dimensional lattices, or a discrete structure, in which the subunits form either rings or a highly symmetrical 3-dimensional assembly, generally referred to as a 'protein cage'. In all of these cases the structures can be mathematically described by a combination of rotational and translational symmetry operations that map one subunit on to any of the others.

Naturally occurring one-dimensional protein fibers include the well-studied proteins actin and tubulin, which play vital structural roles in the cell. Actin (Fig. 8.1a) is one of the most common fiber-forming proteins, and is found in high abundance in nearly all eukaryotic cells, where it is the principle component of the cytoskeleton (Dominguez and Holmes 2011). The dynamic polymerization and de-polymerization of actin underpins important mechanical properties in the cell such as motility, and elongation during cell division. The cylindrical fibers formed by tubulin are the principle component of the microtubules that form the mitotic spindles responsible for the separation of chromosomes during mitosis. This protein also undergoes dynamic polymerization and de-polymerization (Abal et al. 2003). Inhibition of this process by taxanes forms the basis for these drugs' potent anti-cancer activity. Taxane-capped microtubules are unable to depolymerize, effectively inhibiting mitosis without causing immediate cell death.

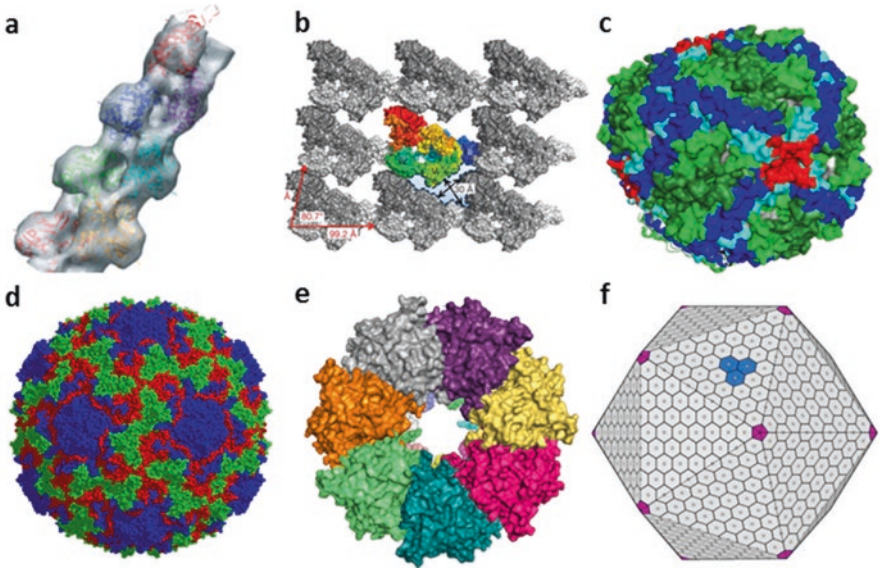

Fig. 8.1 Natural protein cages. (**a**) Cryo-EM reconstruction of fibrous actin (Adapted with permission from Oda et al. 2009, © Macmillan Publishers Ltd) (**b**) Crystal structure of an S-layer protein lattice with *P4* symmetry (Adapted with permission from Baranova et al. © Macmillan Publishers Ltd, 2012) (**c**) Crystal structure of octahedral bacterioferritin (PDB ID 3GVY) (**d**) Crystal structure of icosahedral rhinovirus capsid (PDB ID 4RHV) (**e**) View along the sevenfold axis of the crystal structure of GroEL (PDB ID 1GRL) (**f**) Cartoon of an assembled bacterial microcompartment consisting of hexameric (*blue*) and pentameric (*purple*) subunits (Adapted with permission from Yeates et al. 2011 © Elsevier)

Two-dimensional protein lattices are probably the least well-known and studied class of protein assemblies. They are found primarily in bacteria and archaea, where they form porous surface layers, or S-layers (Fig. 8.1b) that adhere to the outer layer of the cell wall and can comprise up to 20% of an organism's total protein content (Sára and Sleytr 2000). S-layers comprise multiple copies of one or a few glycoproteins, which can be made to self-assemble *in vitro* into lattices, rods, or spheres (Sleytr and Beveridge 1999). Each species has one or more unique S-layer proteins that form pores with sizes ranging from 2–8 nm. Different S-layers are characterized by different symmetries – so far S-layers have been identified with oblique (*P1* and *P2*), square (*P4*), and hexagonal (*P3* and *P6*) symmetries. These proteins are thought to play a role in such critical cellular functions such as cell adhesion, molecular sieving, and binding of toxic cations. Several species of bacteria have been found to synthesize different S-layer proteins in response to environmental stress, suggesting that S-layers may play a role in cellular adaptation as well (Sara et al. 1994).

Three-dimensional protein cages are characterized by a high degree of symmetry and are widely distributed in Nature. These play important roles in the storage of nucleic acids and iron, in protein folding and in confining reactive intermediates in

metabolism. A key feature of protein cages is their ability to create a unique microenvironment within the cage interior that determines the cage's function. A good example is the iron storage protein ferritin (Theil 1987). This octahedral, 24-subunit protein cage is highly conserved and found in almost all organisms (Fig. 8.1c). The interior surface of the ferritin cage contains a large number of negatively charged residues. These bind ferrous iron atoms and catalyze their oxidation to the ferric form and thence to ferric oxide, which in turn serves as a nucleation site for other iron atoms. Additional nucleation of iron continues until the interior of the ferritin protein cage is completely filled with as many as 4500 iron atoms. This allows the cell to store iron, a biologically scarce element, in a highly efficient manner compared to a protein with discrete iron binding sites.

Many viruses encapsulate their DNA or RNA in an icosahedral protein capsid that is built from multiples of 60 protein subunits (Fig. 8.1d). In contrast to ferritin, the interior-facing residues of capsid subunits are positively-charged, thereby neutralizing the negatively charged nucleic acids and allowing them to be efficiently packaged within the capsid. Viral capsids also nicely illustrate another feature of protein cages – highly cooperative assembly of the subunits. Whereas binding interactions between individual subunits are usually much weaker than most protein-protein interactions, dissociating a single subunit from an assembled capsid requires significantly more energy (Singh and Zlotnick 2003). This cooperative binding effect imbues the capsid with a high degree of stability and protects the capsid proteins and enclosed nucleotides against environmental degradation (Ross et al. 2006).

Chaperonins, also known as heat shock proteins, illustrate the use of protein cages to create unique reaction environments, in this case to facilitate refolding of misfolded proteins (Vabulas et al. 2010). Most chaperonins form protein complexes with various symmetries including one of the only known tetrahedral protein complexes, but all with hydrophobic patches in the interior microenvironment that facilitates the refolding or degradation of misfolded proteins. The GroEL/GroES system is the best studied chaperonin, GroEL forms a barrel-shaped 14-subunit protein cage with a 4.5 nm wide hydrophobic interior channel (Fig. 8.1e), with heptameric GroES serving as a 'lid' for the barrel. Misfolded proteins bind to the hydrophobic interior of the barrel, followed by an ATP-driven conformational change in the GroEL subunits, which results in the interior surface becoming significantly more polar and pulling the misfolded protein apart. The unfolded protein then has the opportunity to refold correctly in the sequestered environment provided by the protein cage (Landry and Gierasch 1991).

Bacterial microcompartments (BMCs) provide another good example of a protein cage designed to facilitate biological reactions. BMCs comprise hexameric shell proteins that form a honeycomb-shaped lattice, interspersed with a small number of pentameric shell proteins that introduce kinks into the lattice (Yeates et al. 2008). The combination of hexamers and pentamers yields large (40–200 nm in diameter) pseudo-icosahedral protein complexes (Fig. 8.1f) capable of co-encapsulating multiple enzymes in a metabolic pathway to increase the efficiency of catalysis. The best-studied BMC is the carboxysome, found in photosynthetic cyanobacteria, which co-encapsulates carbonic anhydrase and RuBisCo. Carbonic

anhydrase produces CO_2 from bicarbonate, which is quickly reacted with ribulose bisphosphate by RuBisCo as part of the Calvin cycle. Delocalizing carbonic anhydrase to the cytosol results in significant loss of RuBisCo efficiency (Price and Badger 1989), indicating that the carboxysome plays an important role in the efficient fixation of CO_2 by cyanobacteria.

8.3 Applications of Natural Protein Assemblies

8.3.1 Functionalization of Protein Cages

Naturally-occurring protein assemblies have been adapted for use in a diverse range of materials science and nano-medicine applications. The simplest functionalization of a protein assembly involves modifying the assembly to perform tasks similar to its cellular function. The natural ability of ferritin to biomineralize iron salts to form iron oxide nanoparticles of a defined size has been exploited to synthesize a wide variety of nanoparticles including silver, platinum, palladium, cobalt oxide, and cadmium sulfide (Flenniken et al. 2009). In the presence of a small peptide fragment a ferromagnetic nanoparticle of CoPt could also be synthesized (Klem et al. 2005). Biomineralization functionality could also be engineered into heat shock proteins (McMillan et al. 2005; Ishii et al. 2003) and viral capsids (Brumfield et al. 2004) by mutating the hydrophobic or cationic interior of these proteins to metal-binding or anionic residues. This allowed highly mono-disperse iron oxide nanoparticles to be synthesized with sizes determined by the interior diameter of these protein cages. These protein cage-derived iron-oxide nanoparticles could then be used as a nucleation site for the synthesis of single-walled carbon nanotubes, with the diameter of these nanotubes being proportional to the size of the seed iron oxide particle (Kramer et al. 2005).

Precisely sized nanoparticles, in particular iron and cobalt oxide, are of considerable interest in nanoelectronics research (Jutz et al. 2015). A single layer of protein cages containing nanoparticles can be deposited onto a pre-coated surface in a tight, hexagonal packing pattern, with a packing density close to theoretical values (Atsushi et al. 2006). In what is known as the bio-nano process, silicon wafers or other substrates are precisely patterned with hydrophobic or hydrophilic coatings, with nanoparticle-containing ferritin localizing only on the hydrophilic film. This is then exposed to heat, burning away the ferritin to leave only the iron oxide nanoparticle, which is then reduced to yield a precisely-patterned array of metallic iron spheres (Takuro et al. 2007). This has been used to generate semiconducting logic devices on the nano scale such as thin film transistor flash memory and floating nanodot gate memory devices (Kazunori et al. 2007). Parameters of the bio-nano process can be controlled with superior precision than existing nanoelectronics technology (Kiyohito et al. 2007) although this technology has not yet found a commercial application.

The microenvironment of the protein cage interior presents an attractive target for entrapping catalytic species, thereby creating a nano-scale bioreactor (Bode et al. 2011). Palladium nanoparticles formed on the interior of ferritin have been shown to catalyze the hydrogenation of olefins (Ueno et al. 2004). The kinetics of this reaction could be controlled by varying the size of the olefin substrate, indicating that this reaction is limited by diffusion of the olefin through the pores of ferritin. Similarly a rhodium (II) complex bound to the interior of ferritin was used to catalyze the polymerization of phenylacetylene (Abe et al. 2009). The resulting polymer, encapsulated within the ferritin cage, had a remarkably narrow size distribution. This level of precision in polymerization control may open up new avenues of research into designed smart materials.

The hollow interior of a protein cage has also sparked interest for entrapment and immobilization of enzymes, fashioning a bioreactor similar to the carboxysome. Protein cages can be assembled around enzymes in solution, trapping them, and these enzymes retain their catalytic activity (Comellas-Aragones et al. 2007). Using one of the larger viral capsid shells, multiple enzymes in a metabolic pathway were co-localized, but this had negligible effect on turnover rates (Patterson et al. 2014a), and there are indications that the catalytic activity is actually reduced due to crowding effects when a large number of enzymes are encapsulated in each protein cage (Minten et al. 2011).

Protein cages also hold promise for biomedical applications. Viral capsids, i.e. protein cages lacking the viral genome, are a particularly attractive target for therapeutic delivery systems, as the viral capsid has evolved to cross the cell membrane and deliver its payload. The sizeable interior cavity of a viral capsid has been adapted to encapsulate drug molecules and imaging agents, and can also accommodate plasmids as large as 17.6 kbp, thereby protecting them from nucleases (Kimchi-Sarfaty et al. 2003; Štokrová et al. 1999). An exotoxin-encoding plasmid encapsulated in a viral capsid was delivered in this way to tumor cells, resulting in a reduction of the size of the tumor *in vivo* (Kimchi-Sarfaty et al. 2006). Likewise, small molecules that are encapsulated in the capsid interior or covalently bound to the protein cage can be delivered to the cells with greater efficiency than unmodified small molecules (Aljabali et al. 2013), and can be released over an extended period of time (Flenniken et al. 2005).

Using protein cages as a delivery vehicle for therapeutics still has the drawback that their toxic payload is delivered indiscriminately. Therefore significant research has gone into decorating the capsid exterior with targeting ligands that localize the therapeutic protein cage to the cell type of interest. Drugs can be selectively targeted to specific cell types by decorating viral capsids with either small molecules (Zhao et al. 2011; Banerjee et al. 2010) or large biomolecules (Huang et al. 2011; Lockney et al. 2011) that bind receptors that are overexpressed by many cancer cell types. For example, by engineering appropriate receptor-targeting sequences onto the exterior of the capsid, therapeutic molecules could selectively target Jurkat leukemia T cells (Stephanopoulos et al. 2010) or human hepatocellular carcinoma cells (Ashley et al. 2011). In both cases, the protein cages delivered their cytotoxic payload exclusively

to the targeted cells, inducing cell death in the majority of those cancer cells without affecting any of the control cells.

Protein cages also hold promise for therapeutic imaging *in vivo* by encapsulating positron emission tomography (PET) imaging agents or magnetic resonance imaging (MRI) contrast agents (Cormode et al. 2010). The common PET imaging agent ^{18}F was bioconjugated to viral capsids (Hooker et al. 2008) and the location of these capsids could be dynamically imaged *in vivo* (Flexman et al. 2008). Iron oxide nanoparticles, a simple and effective MRI contrast agent, could be inserted into the hollow cavity of ferritin (Uchida et al. 2008) or viral capsids (Ghosh et al. 2012) with similar results. Notably, incorporation of Gd^{3+} into the calcium-binding sites of the cowpea chlorotic mosaic virus led to a species with the highest relaxivity values measured to date, potentially leading to new applications with low-dose MRI contrast agents (Allen et al. 2005).

Viral capsids have a tendency to elicit strong immunogenic responses due to the display of multiple epitopes on the capsid surface (Kaiser et al. 2007). Whereas this is a disadvantage for many applications, it has attracted significant interest in the field of vaccine development. Recombinantly-produced viral capsids induce a strong immune response while offering a safe alternative to the use of attenuated or killed virus particles as they contain no genetic information from the virus; the major concern being that this immunogenicity must be modulated to avoid an adverse immune response (Rebeaud and Bachmann 2012; Jennings and Bachmann 2009). They also obviate the use of toxic adjuvants such as aluminium that are needed to boost immune response when low-copy epitopes are used as vaccines (Kawano et al. 2013). Currently over a dozen capsid-based vaccines are approved for clinical trials or clinical use, targeting Influenza, Hepatitis A & B, HPV, and others (Teunissen et al. 2013; Donaldson et al. 2015). Most interestingly, viral capsids have shown promise as vectors for therapeutic vaccinations against non-viral diseases, such as Alzheimer's disease (Wiessner et al. 2011), cancer (Garcia 2011; Speiser et al. 2010), arthritis (Spohn et al. 2008), and nicotine addiction (Maurer et al. 2005).

8.3.2 Functionalization of S-Layer proteins

Bacterial S-layer proteins have also been explored for functionalization, although the extended geometry results in different capabilities. Like protein cages, assembled S-layers have interfacial pores, which can be modified to biomineralize a broad range of metal ions (Mertig et al. 1999; Shenton et al. 1997). However, unlike protein cages, S-layers lack a defined interior or exterior, instead surface residues can be categorized based on which face of the assembled S-layer it resides. One face of the S-layer is strongly cytophilic due to the presence of several homologous 4-residue long sequences which bind to cell wall-associated peptidoglycans, while the other face of the S-layer is strongly cytophobic (Engelhardt and Peters 1998).

For one of the best-studied S-layer proteins, SbpA from *Lysinibacillus sphaericus*, it was discovered that the orientation of the faces was dependent on the pH of the solution during deposition: basic or neutral solutions induce SbpA to crystallize with the cytophobic face exposed, whereas acidic solutions induce crystallization with the cytophilic face exposed (Rothbauer et al. 2013). This property was used to design antifouling (cytophobic) ultrafiltration membranes (Weigert and Sára 1996). Co-immobilizing proteins such as glucose oxidase (Picher et al. 2013) or a prostate-specific antigen (PSA) antibody (Pleschberger et al. 2004) to the cytophobic face of the S-layer allowed metabolites such as glucose and prostate-specific antigen to be accurately detected. This method gave significantly lower rates of false positives due to nonspecific cell adhesion than standard methods such as adhesion to gold nanoparticles. Ligands that bind specific cell types have also been attached to the cytophobic face of an S-layer, and by controlling the deposition of several orthogonally mutated S-layers, co-cultures of different cell types could be obtained in a spatially defined manner (Rothbauer et al. 2015).

S-layers can also be functionalized for therapeutic aims, although they have been utilized much less extensively than protein cages. Due to their repetitive structure, S-layers induce a heightened immune response, but are generally regarded as less effective than other methods of epitope presentation (Ilk et al. 2011). However, purified S-layers can be used to inoculate against the species of bacteria that produces the S-layer. This approach was used to generate an effective vaccine against six virulent isolates of the fish pathogen *Aeromonas hydrophila*, which was otherwise very difficult to vaccinate against due to the wide variation between isolated strains (Poobalane et al. 2010).

Bacterial S-layers have also been explored for drug delivery applications. The cytophilic face of SbpA was found to bind to the outer layer of liposomes, encasing them as it would a cell wall (Ucisik et al. 2015). This dramatically increased the shelf life of liposome-based therapeutics by reducing the rate that the drug molecules diffused through the liposome, a common limitation of liposome-based therapies (Raza et al. 2013). The S-layers on encased liposomes are functionalizable – by genetically fusing an eGFP sequence to the terminus of an S-layer, individual liposomes could be observed as they diffused through the cell membrane (Ilk et al. 2004).

8.4 Design of *de novo* Protein Assemblies

Functionalizing natural protein assemblies represents one approach to developing new bio-inspired materials; unfortunately there are a relatively small number of well-characterized natural assemblies amenable to modification. An alternative approach that has gained popularity in recent years is to design protein assemblies *de novo* from multiple copies of smaller symmetric building blocks. The primary advantage of this approach is customizability: depending upon the choice of protein

building block and the manner in which the blocks are assembled, one can introduce a wide range of functionality into the assembly, control the interior cavity size and potentially make its assembly responsive to environmental conditions or specific ligands.

8.4.1 Conceptual Approaches to Protein Assembly

The basic requirements for assembling a protein into a geometrically well-defined structure are deceptively simple: one must have two rotationally symmetric protein domains connected at the proper dihedral angle (Fig. 8.2a) (Yeates and Padilla 2002). For simplicity, we will only discuss the assembly of protein cages, but the principles described below apply to the design of extended protein assemblies as well.

Protein cages formed by connecting two symmetric protein domains can be found in four distinct point symmetries: tetrahedral (T or 332), octahedral (O or 432), icosahedral (I or 532), and prism (D_n). For the first three of these symmetries, any two of the three symmetry operators may be combined at the proper angle to yield a protein assembly with that symmetry. Thus, an icosahedral cage can, in principle, be formed from a subunit possessing domains that oligomerize with the following rotational symmetries: a threefold and a twofold oligomerization domain, a fivefold and a threefold domain, or a fivefold and a twofold domain, although the requisite dihedral angle between the two symmetry axes differs for each of these three "symmetry pairs". The binary permutations of symmetry pairs that can be used to assemble protein cages with tetrahedral, octahedral and icosahedral geometries are illustrated in Fig. 8.2b. In addition, any symmetry pair with a twofold symmetry element also has the potential to form a prism. GroEL, a 14-subunit protein cage formed from a sevenfold and a twofold symmetry pair, serves as an excellent example of this symmetry.

Although it is relatively easy to genetically fuse two protein domains that oligomerize with the desired symmetry to each other, it is the alignment of their respective symmetry axes that has posed the greatest challenge to the successful design of protein cages. This is because protein structures are both inherently asymmetric and flexible. Designing in the correct dihedral angle between two symmetry sites is difficult and requires a high level of precision, as a rigid, but improperly oriented dihedral angle will lead to aggregation. The alternative, allowing the dihedral angle to remain flexible, can lead to a wide variety of possible assemblies with irregular geometries, although the range of structures can be restricted, as discussed below.

For flexible self-assembling systems, in which the dihedral angle between symmetry elements is completely unconstrained, the only constraint is that there must be no unpaired symmetry elements. This means that the set of stable, discrete protein assemblies, in principle, contains almost all of the assemblies with a subunit number that is a multiple of the least common denominator of the two symmetry elements. Thus, a trimer-dimer symmetry pair forms assemblies with multiples of 6

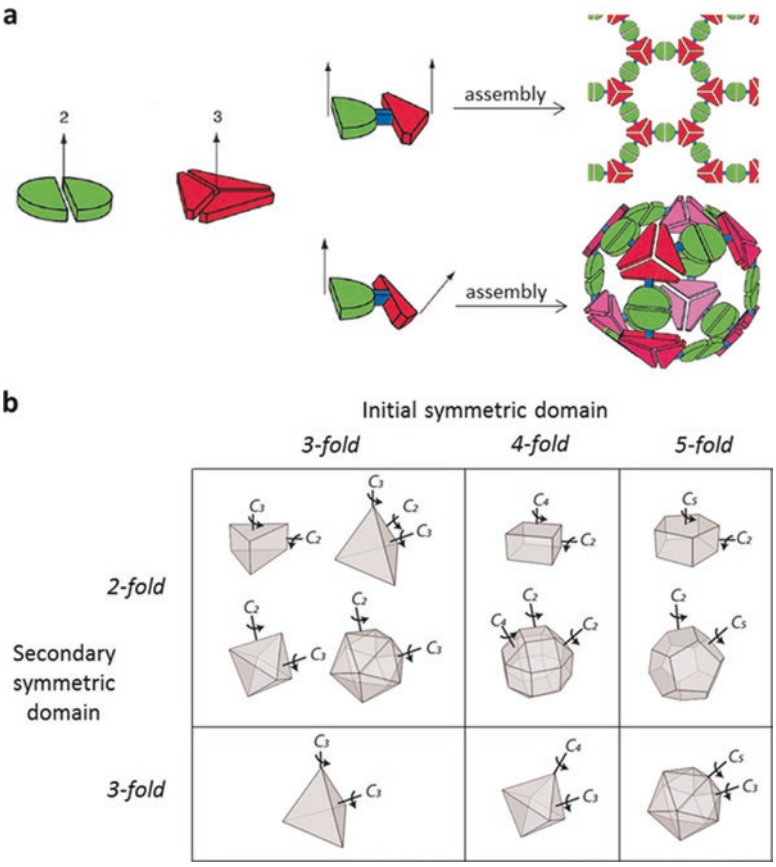

Fig. 8.2 Assembly of designed fusion protein assemblies (**a**) Rigidly linking a dimeric protein (*green*) with a trimeric protein (*red*) will result in different assemblies depending on the dihedral angle imparted by the rigid linker (*blue*) (Adapted from Padilla et al. 2001) (**b**) Six different symmetry pairs of fusion proteins connected at a proper dihedral angle are expected to result in the assembly of closed Euclidean solids

subunits (or 2 trimers), a trimer-trimer symmetry pair forms assemblies with multiples of 3 subunits (one trimer), and a trimer-tetramer symmetry pair forms assemblies with multiples of 12 subunits (4 trimers) (Fig. 8.3).

The specific complexes that can be formed for each symmetry pair is dependent on the range of allowed dihedral angles imparted by the flexibility in the system. For example, one of the possible 16-trimer assemblies formed from a subunit with a trimer-tetramer symmetry pair is arranged like an icosahedron but missing four nonadjacent trimers. If the range of allowed dihedral angles for the subunit of this trimer-tetramer system was restricted to one close to an icosahedron, this 16-mer pseudo-icosahedral species would be favored; whereas the ring-shaped 16-mer of trimers requires a much wider range of dihedral angles to form. While ostensibly,

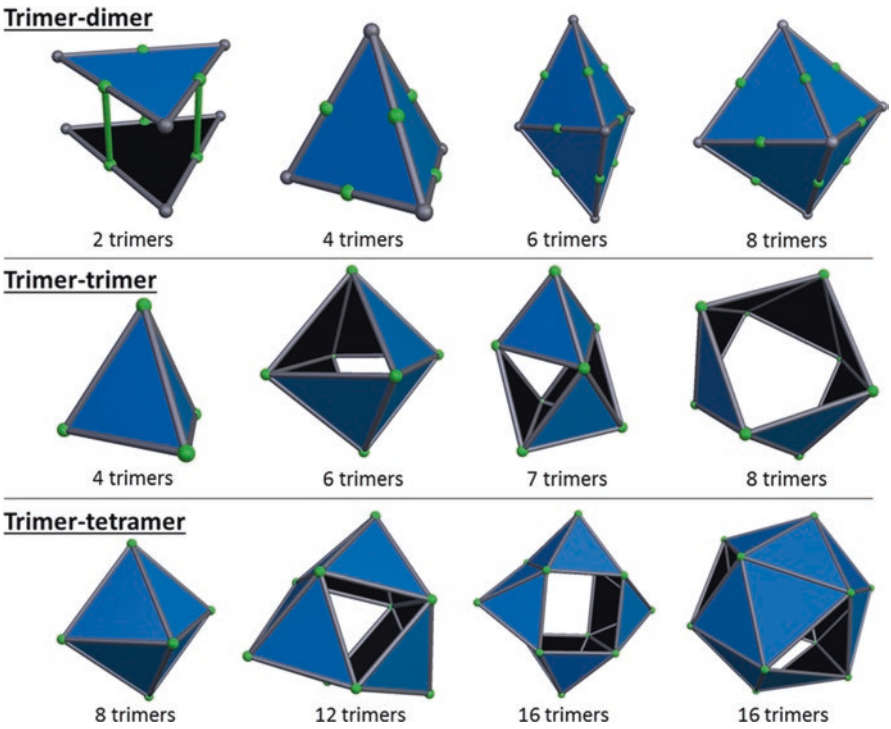

Fig. 8.3 Examples of possible assemblies that can be formed from fusion proteins with different symmetry pairs. *Blue triangles* represent a trimeric building block protein, fused with a second symmetric protein, represented as *green dots* at either the edges (dimeric symmetry domain) or vertices (trimeric or tetrameric symmetry domains) of the *blue triangles*. The assembled structures may be porous and/or require differing dihedral angles to form, but have the correct oligomerization state at every point of attachment and contain no unpaired symmetry elements

the analysis above implies that a flexibly-linked symmetry pair naturally makes an infinite assortment of complexes, in reality smaller assemblies are entropically favored (Boyle et al. 2012). Thus the assembly of the octahedron from a flexibly-linked trimer-tetramer symmetry pair is favored over either of the 16-trimer structures shown in Fig. 8.3.

8.4.2 Extended Assemblies – Designed Fibers and Lattices

The simplest *de novo* designed protein assemblies are one-dimensional protein fiber strands. These only require an asymmetric unit with two different self-associating dimeric interfaces. Since many natural proteins exist as dimers, it is relatively simple to design a fiber-forming asymmetric unit, with the earliest designs dating from the mid-1990s (Zhang et al. 1993; Woolfson 2010). This is because dimer-dimer

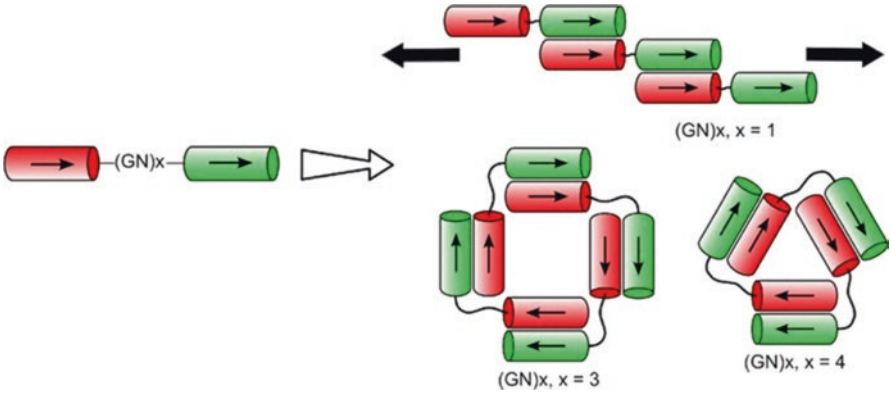

Fig. 8.4 A designed fusion protein with a flexibly-linked dimer-dimer symmetry pair assembles into filaments when this linker is short (*top*) but with longer linkers assembles into discrete oligomers whose size is inversely proportional to the length of the flexible linker (*bottom*) (Reprinted with permission from Boyle et al. 2012 © American Chemical Society)

symmetry pairs can still assemble into fibers even if the two dimeric domains aren't precisely oriented opposite to each other. In the general case, these assemblies form helical structures at the micro level, but still results in the formation of a fibrous macrostructure. These fibers can form networks that give rise to interesting solution-phase properties, such as hydrogelation (Rajagopal et al. 2009; Dong et al. 2008) and antibacterial activity (Salick et al. 2007; Ghadiri et al. 1993), and have been investigated as substrates for cell adhesion and growth (Haines-Butterick et al. 2007; Villard et al. 2006).

The formation of fibers requires a degree of rigidity between the oligomerization domains, otherwise the ends of the fiber will close on each other to form rings. This is illustrated clearly by a designed, rigid filament-forming fusion protein that was modified by adding a flexible linker between its two dimerization domains (Boyle et al. 2012). The protein assembly retained its filamentous structure after 2 or 4 flexible residues were added, but with the addition of a 6-residue linker the protein assembled into a tetramer-of-dimers, while an 8-residue linker yielded a trimer-of-dimers, and 10 residues led to a mixture of trimers-of-dimers and dimers-of-dimers (Fig. 8.4).

The fusion protein approach has also been used to design two-dimensional lattices; this is a harder problem due to the extra spatial dimension that must be aligned. In an early study a cysteine residue was introduced at each edge of a fourfold symmetric aldolase protein, allowing it to be tagged with biotin (Ringler and Schulz 2003). The dimeric, biotin-binding protein streptavidin was then mixed with the modified aldolase, resulting in a square lattice-like assembly. However, the lattice could only be propagated for a few repeating units before becoming disordered. A later study that examined the assembly of five different tetrameric proteins when fused to a streptavidin tag found that two of these five could be assembled into lattices that maintained order over a large number of subunit repeats (Fig. 8.5) (Sinclair

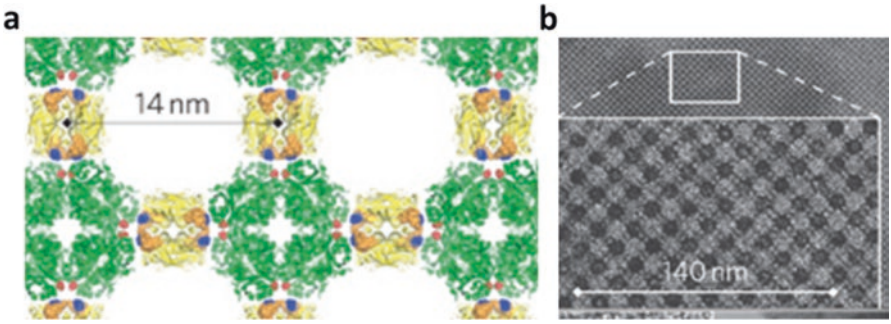

Fig. 8.5 A *de novo* designed square lattice (**a**) Designed lattice assembled by connecting a four-fold and a twofold-symmetric protein (**b**) TEM image of the assembled lattice (Adapted with permission from Sinclair et al. 2011, © Macmillan Publishers Ltd)

et al. 2011). For one protein lattice, assembly was found to be dependent on the linker length;: a linker of less than two residues resulted in nonspecific aggregation, but a two or three residue linker formed long-range lattices.

In a different approach, a two-component system based on *de novo* designed coiled-coils was constructed by linking a homo-trimeric coiled-coil to one of two heterodimer-forming α-helices through a disulfide bond (Fletcher et al. 2013). The locations of the two cysteine residues were chosen to orient the two oligomerization domains back-to-back, such that the resulting lattice would form a two dimensional honeycomb pattern as illustrated in Fig. 8.6. Instead, due to the slight inherent flexibility of proteins, these fusion proteins formed hollow spherical assemblies approximately 100 nm in diameter, similar in kind to bacterial microcompartments (Fletcher et al. 2013). Interestingly, a mutation of Asn to Ile introduced at the heterodimeric interface that increased the binding affinity of the heterodimeric coiled-coil resulted in particles forming with a 33% smaller diameter. This illustrates the interplay between thermodynamic forces in protein assembly – strengthening the coiled-coil interaction allows the proto-particle to overcome larger steric stresses associated with increasing the curvature of the honeycomb lattice and thus forms smaller particles.

Advances in computational methods have allowed more precisely designed protein lattices to be constructed. Lanci et al. generated a protein crystal with the rarely-observed space group *P6* by computationally designing a self-dimerizing interface into the outwardly-facing side-chains in a homo-trimeric coiled-coil (Fig. 8.7) (Lanci et al. 2012). A different hexagonal lattice was designed from a hexameric building block protein (Fig. 8.8) (Matthaei et al. 2015). After computationally aligning hexamers into the desired lattice, the inter-terminus distance was measured between subunits of adjacent hexagons. Using this as a guide, a linker was designed that was long enough to bridge between adjacent hexagons, but too short for both subunits of the fusion protein to fit into the same hexagon.

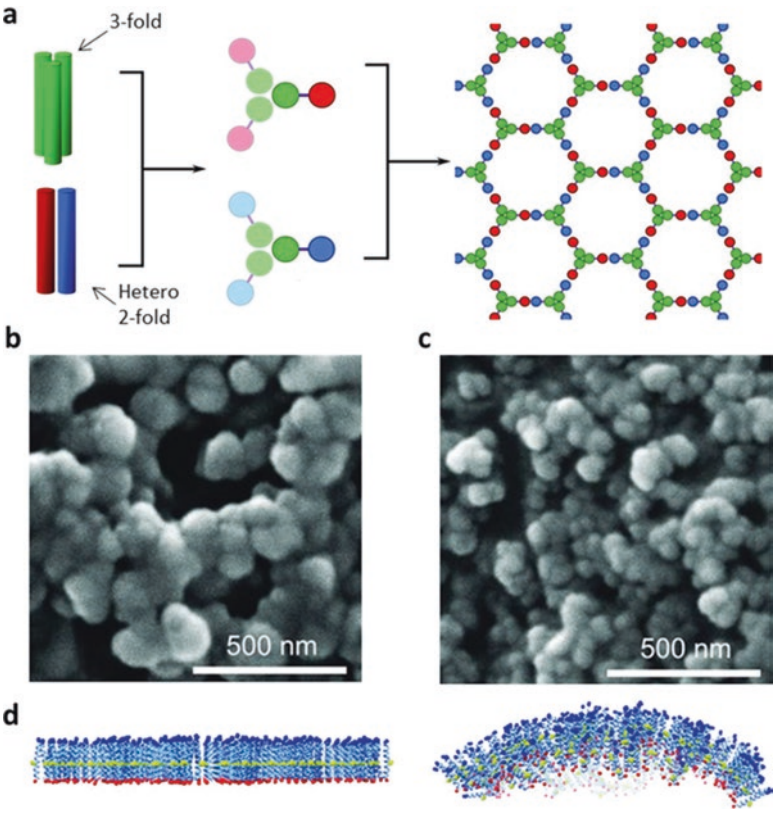

Fig. 8.6 Assembly of bacterial microcompartment-sized spheres from a flexible lattice-forming protein. (**a**) Design scheme: A homo-trimeric coiled-coil (*green*) was attached to one of two halves of a heterodimeric coiled-coil (*red* & *blue*), which combine to make a hexagonal lattice. (**b**, **c**) SEM images of the assembled superstructure with a weakly-associating (**b**) or a strongly-associating (**c**) heterodimer. (**d**) *Side view* of the molecular dynamics simulation of the potential curvature across 19 tessellated hexagons (Figure reproduced with permission from Fletcher et al. 2013, © American Academy for the Advancement of Science)

The Tezcan group has focused on the design of split metal-binding sites to mediate protein assembly. Each protein subunit supplies half of the ligands to the metal, typically Zn^{2+}, which bridges between the two subunits (Brodin et al. 2012). Computational design was used to position two Zn-mediated dimerization domains orthogonally to each other, with one domain having a significantly higher affinity than the second. Addition of one equivalent of Zn^{2+} resulted in dimerization in solution, as predicted, but the crystal structure of the dimeric complex revealed that there was a third, weak oligomerization site that connected two neighboring dimers together, such that they formed a zigzag-shaped chain (Fig. 8.9a). After a second equivalent of Zn^{2+} was added, dimerization occurred at the low-affinity site and the protein assembled into a 2-dimensional lattice. Interestingly, adding a large excess

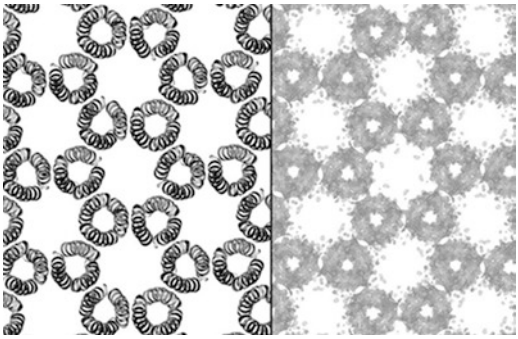

Fig. 8.7 Trimer-dimer system designed to form a protein crystal with the *P6* space group. Computational model (*left*) matches well with the cryo-EM reconstruction (*right*) (Figure adapted from Lanci et al. 2012)

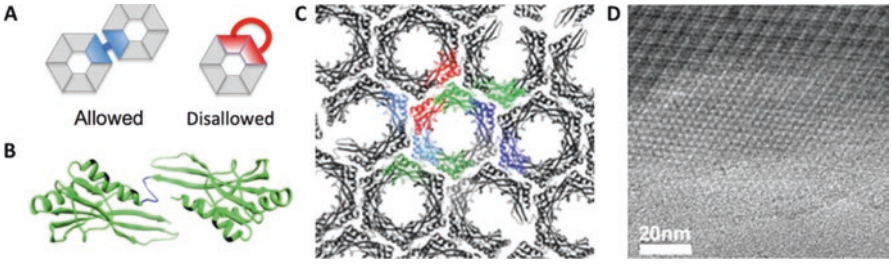

Fig. 8.8 Computational design of a flexibly-linked lattice. (**a**) Design scheme: The flexible linker must be long enough to connect two protein subunits on adjacent hexagons but not long enough to connect two protein subunits on the same hexagon. (**b**) The designed fusion protein comprising two subunits connected by a six glycine linker. (**c**) The predicted hexagonal lattice structure. Six fusion proteins comprising a single hexagon are colored separately. (**d**) TEM image of the assembled lattice (Figure adapted from Matthaei et al. 2015 © American Chemical Society)

of Zn^{2+} (>100 equivalents) or increasing the pH from 5.5 to 8.5 caused the formation of nanotubes (Fig. 8.10b). Most likely this was due to the increased binding affinity driving the assembly of smaller structures over the effects of steric hindrance, as discussed previously. Introduction of a cysteine residue at a position orthogonal to the two-dimensional lattice allowed these lattices to be further assembled into three-dimensional microcrystalline arrays using a dimaleimide cross-linker.

Interestingly, lattices have even been designed by using a natural protein cage as the building block. Yang et al. used ferritin as a building block to generate a square lattice, linking two adjacent ferritin nanoparticles together with a strand of poly(L) lysine, which was long enough to bind to the anionic interiors of two adjacent ferritin cages and bridge the gap between them (Fig. 8.10) (Yang et al. 2014). To accomplish this, the ferritin building blocks had the C-terminal α-helix removed, which widened the pore at the fourfold axis and allowed the poly(L)lysine connecting chain to pass into the cage interior. This ensured that the ferritin nanoparticles were aligned solely along their fourfold symmetry axes.

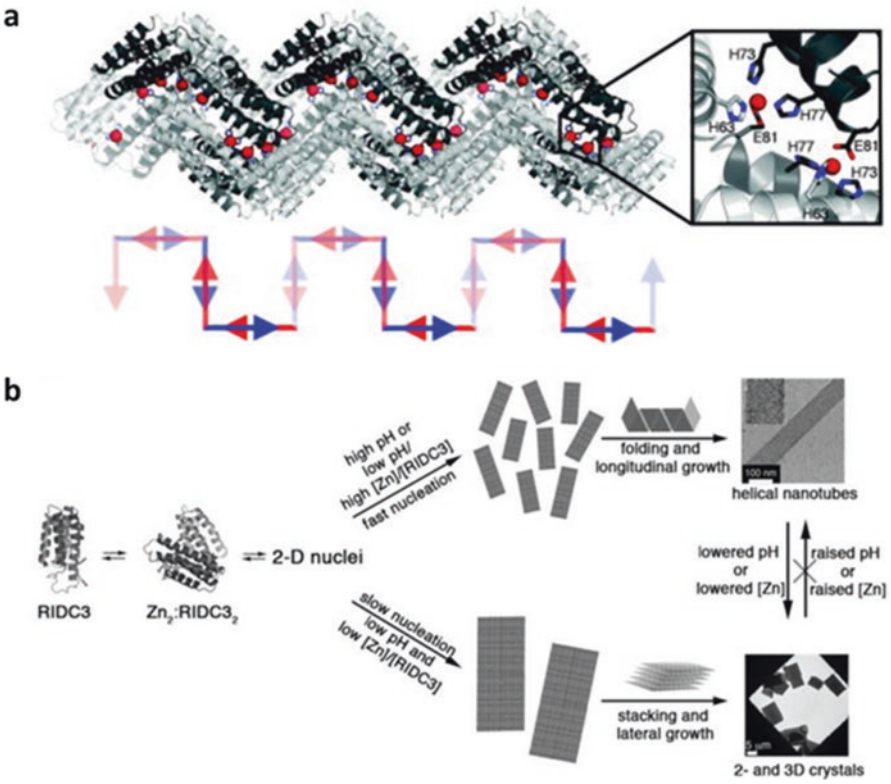

Fig. 8.9 Design of a lattice with multiple orthogonal Zn-mediated binding sites. (**a**) Crystal structure of the assembly after one equivalent of Zn was added. Instead of forming a homodimer as expected, 1-D arrays were generated due to weak dimer-dimer interactions. (**b**) The formation of different macrostructures is dependent on the ratio of excess Zn to protein (Adapted with permission from Brodin et al. 2012, © Macmillan Publishers Ltd)

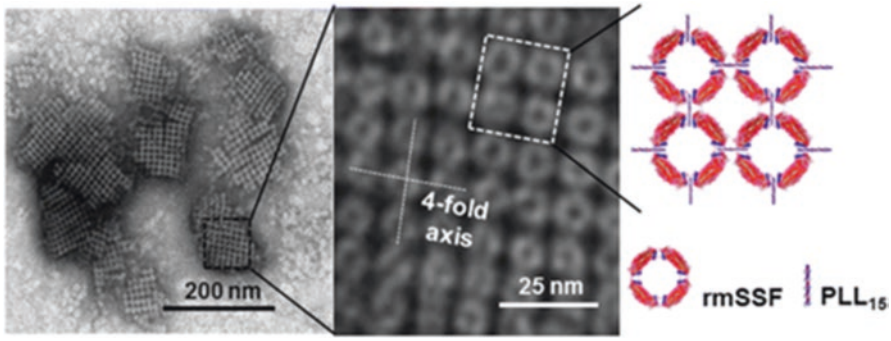

Fig. 8.10 A ferritin-based square lattice. TEM image depicts ferritin protein cages assembled into a *square lattice* by way of a poly(L)lysine linker (Reproduced from Yang et al. 2014 with permission of The Royal Society of Chemistry)

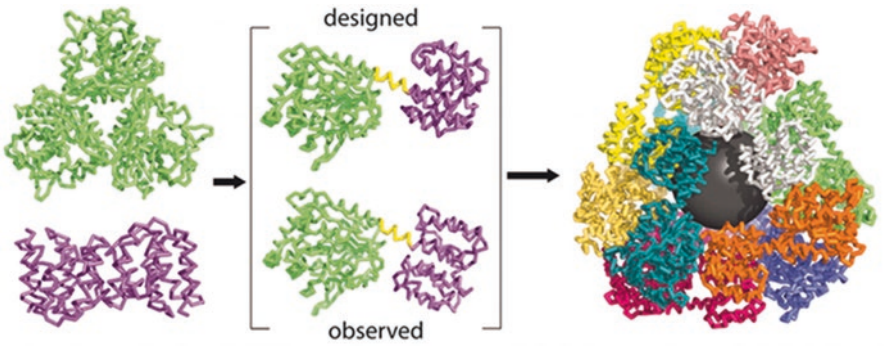

Fig. 8.11 Crystal structure of a *de novo* designed tetrahedral protein cage. While the designed subunits had a rigid α-helix connecting the trimeric and the dimeric domains, the crystal structure (*right*) shows considerable torsion between domains (Adapted with permission from Lai et al. © Lai et al. 2012 MacMillan Publishing Ltd)

8.4.3 Discrete Assemblies – Designed Protein Cages

In a pioneering study in 2001, Padilla et al. reported the design of a tetrahedral protein cage by linking a trimeric protein domain to a dimeric protein domain, through a rigid alpha helical linker sequence (Padilla et al. 2001). The linking α-helix extended between the C-terminal α-helix of the trimeric domain and the N-terminal α-helix of the dimeric domain, thereby maintaining a rigid connection. This allowed the dihedral angle between the two symmetric domains to be modified in a stepwise manner by adding or removing residues in the linking segment, with each additional residue twisting the dihedral angle by 100°. For the two symmetric protein domains used, a nine-residue α-helical linker was predicted to be close enough to orient the dihedral angle for tetrahedron formation. The resulting protein cages appeared tetrahedral when imaged by electron microscopy and had a molecular weight corresponding approximately 12 subunits, as judged by analytical ultracentrifugation. A later simulation of this assembly revealed that two residues from one domain interfered with the intended helix alignment (Lai et al. 2012). When these were mutated to helix-promoting residues the resulting assembly was significantly more homogeneous, and a crystal structure could be obtained. The crystal structure revealed significant torsion between the two oligomerization domains and a deviation of 8 Å from perfect tetrahedral geometry. Nevertheless the design assembled primarily as intended, unintentionally illustrating the benefits of retaining some flexibility in designing protein complexes (Fig. 8.11).

A variation of this design involved shortening the rigid α-helical linker from 9 to 4 residues, which aligned the dihedral angle between the trimeric and the dimeric protein domain to approximately 35°, the angle required for formation of a cubic structure (Lai et al. 2014). After optimization of this 4-residue linker region, the fusion protein assembled into 24-subunit cubes (40% of all assemblies), but also into 18-subunit trigonal bipyramids (50%) and 12-subunit tetrahedrons (10%) (Fig. 8.12).

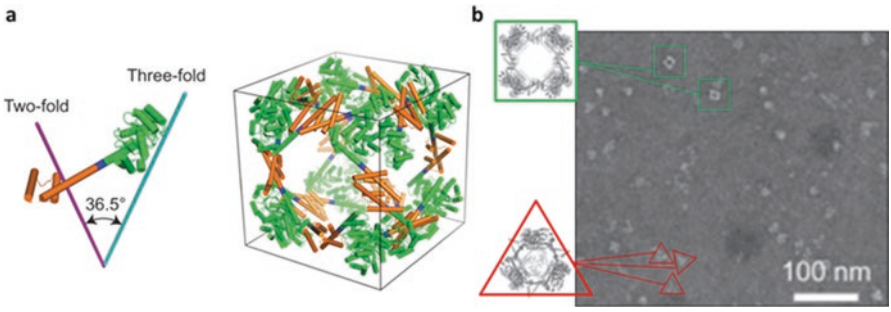

Fig. 8.12 A rigidly-linked trimer-dimer symmetry pair designed to assemble into a 24-subunit cube. (**a**) Model of the intended 24-subunit protein cube. (**b**) TEM of the heterogeneous mixture of assemblies formed. Complexes with apparent octahedral geometry are labeled with *green squares*, while smaller complexes are denoted with *red triangles* (Adapted with permission from Lai et al. 2014, © Macmillan Publishing Ltd)

This polymorphism appears to be a result of the innate flexibility of proteins as well as the tendency for tightly-associated super-symmetric protein subunits to favor smaller assemblies over larger ones, as discussed above. Despite this polymorphism, it was possible to obtain a single crystal of the assembled complex from a carefully purified sample that grew from the crystallization buffer after six months. The x-ray structure revealed that it formed a highly porous cubic structure that closely matched the intended design.

In a different approach, Patterson and coworkers designed two complementary building blocks based upon a trimeric protein, in which two complementary alpha-helical sequences, designed to form an anti-parallel, hetero-dimeric coiled-coil when mixed together, were appended to the N-termini of the protein through a long, flexible linker (Patterson et al. 2011, 2014b). The purpose of these studies was to explore the range of structures that could form in a system where the dihedral angle between the oligomerizing domains was completely unconstrained. Interestingly, upon mixing, the complementary trimeric building blocks assembled into a relatively small range of complexes, despite the unconstrained nature of the design. Analytical ultracentrifugation indicated that the system formed only six different complexes in significant concentrations, with the three major complexes having hydrodynamic properties consistent with the formation of protein cages with diameters appropriate for trigonal prism, tetrahedral or octahedral protein cages. Cryo EM analysis of the particles indicated that they varied in diameter in an almost continuous manner suggesting that their structures were extremely flexible, consistent with the design (Fig. 8.13).

A slightly different approach was taken by Kobayashi and coworkers, who attached a protein sequence comprising two helices of an antiparallel homo-dimeric 4-helix coiled-coil domain to a trimeric building block protein through a flexible linker (Kobayashi et al. 2015). In this case, because the coiled-coil was homo-dimeric, the proteins assembled into cages *in vivo*. This system also formed a mixture of assemblies expected for a trimer-dimer system, with the 6-, 12-, and

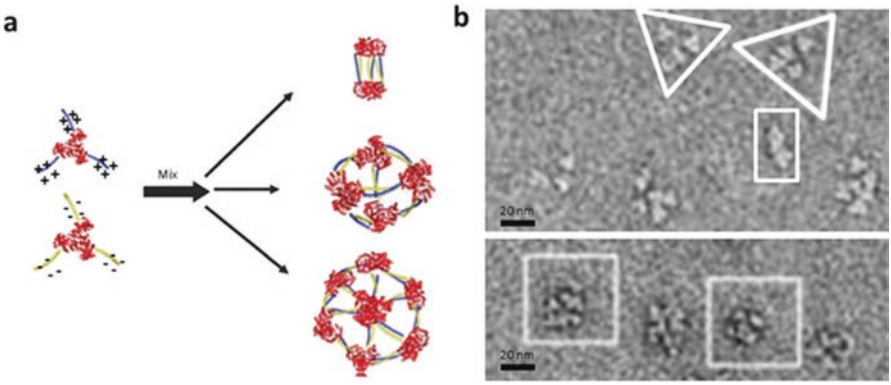

Fig. 8.13 Design of an extremely flexible self-assembling protein cage. (**a**) Design principle: the homo-trimeric building block was linked to an **α**-helix bearing either a strong positive or negative charge. The combination of the two should yield a variety of symmetries. (**b**) TEM of smaller assemblies (*top*) and of larger assemblies (*bottom*) after stoichiometric mixing and size exclusion purification (Adapted from Patterson et al. 2011, with permission from The Royal Society of Chemistry)

18-subunit assemblies able to be purified from the mixture by size exclusion chromatography.

Burkhard and co-workers have explored a cage-forming system that uses a pentameric symmetry element. This system comprises a pentamer-forming coiled-coil linked to a trimer-forming coiled-coil through a two glycine spacer, with the aim of assembling an icosahedral complex (Fig. 8.14) (Raman et al. 2006). To align the two oligomerizing coils with the correct dihedral angle for icosahedral formation, a cysteine residue was inserted on either side of the glycine linker that when oxidized to a disulfide bond would act as a staple. As expressed, this symmetric protein assembled into nonspecific complexes with a broad range of molecular weights. A more homogeneous preparation could be obtained by reducing and denaturing the protein with urea, followed by oxidation and a slow refolding. The refolded protein assembled into fairly homogeneous, spherical complexes of approximately 45 subunits at low concentrations (< 0.3 mg/ml), and approximately 60 subunits at higher concentrations. Interestingly, a variant of this design that substituted the two cysteine residues with alanine formed no 60-subunit icosahedral complexes. Instead, it formed a mixture of spherical assemblies with approximately 180, 240, 300, or 360 subunits, depending on the preparative conditions and the peptide sequence of the asymmetric unit (Indelicato et al. 2016; Yang et al. 2012). These studies clearly depict the challenge of designing well-defined assemblies with higher order symmetry elements.

Although structurally poorly defined, these protein assemblies were able to generate powerful immune responses similar to that of attenuated live viruses, and the intensity of this response could be modulated by changing the diameter of the assembled particles (Yang et al. 2012). This property was exploited to create

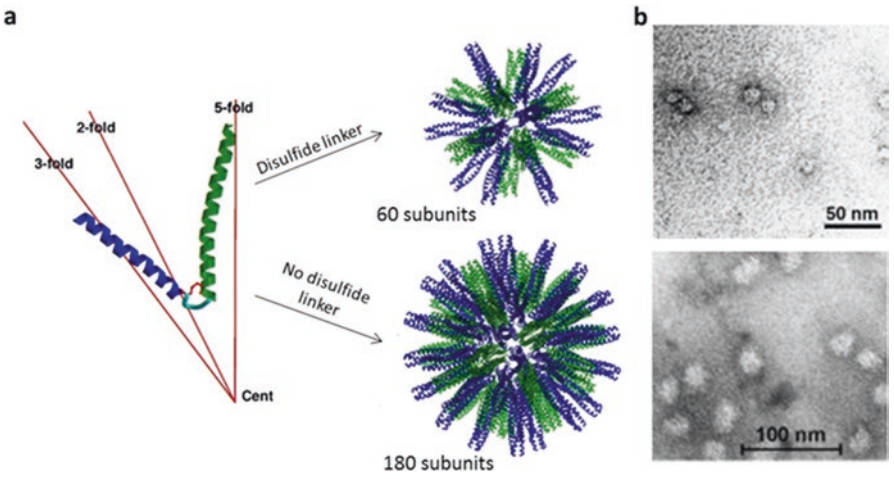

Fig. 8.14 Design of an icosahedral protein cage. (**a**) A protein subunit with a pentamer-trimer symmetry pair assembles into a 60-subunit icosahedron when a disulfide bond is present to lock the dihedral angle in place, but assembles into larger structures in its absence. (**b**) STEM images of the assemblies with (*top*) and without (*bottom*) the disulfide bond present (Adapted with permission from Yang et al. 2012, and Raman et al. 2006, © Elsevier)

functional mouse vaccines for malaria (Kaba et al. 2009), HIV (Wahome et al. 2012), influenza (Babapoor et al. 2011), and toxoplasma (El Bissati et al. 2014) by displaying the respective viral epitope at the terminus of each subunit, which induced long-lasting immune responses to each of these viruses without requiring the addition of an adjuvant.

Advances in computational methods, in particular the program Rosetta developed by Baker and coworkers, have resulted in some impressive advances in the design of *de novo* assembled protein cages. The Rosetta program rapidly and robustly models different docking conformations of protein-protein interfaces, using a built-in scoring function that assesses the energetic stability gained from burying hydrophobic surface residues and creating hydrogen bonds as well as the destabilizing effects of steric clashes and unfavorable Coulombic interactions. Analysis of docked protein interfaces with Rosetta has been used to predict the oligomerization state and binding surface of a self-associating protein from its crystal structure (André et al. 2007; Das et al. 2009). Additionally, new protein-protein interactions can be designed by remodeling a docked structure to add in inter-protein hydrogen bonds and hydrophobic interfaces (Huang et al. 2007; Jha et al. 2010; Stranges et al. 2011).

King and coworkers used Rosetta to design protein cages by symmetrically replicating the structures of 271 trimeric proteins with their symmetry axes centered perpendicular to the faces of either a tetrahedron or an octahedron (King et al. 2012). These assemblies were then analyzed for steric clashes (backbone atoms within 3 Å of each other) and close contacts (backbone atoms within 10 Å of each other) at the inter-trimer surface (Fig. 8.15a) (King et al. 2012). Each trimer was then simultane-

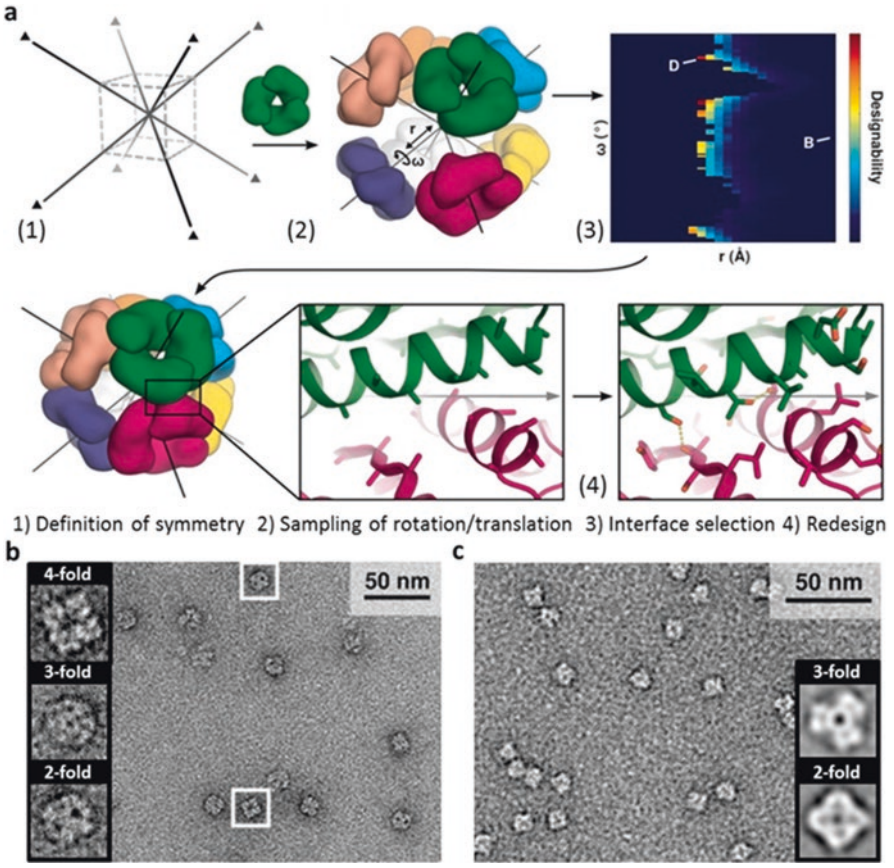

Fig. 8.15 Assembly of protein cages through *de novo* designed protein-protein interfaces (**a**) Outline of design strategy; for details see the text. (**b**, **c**) TEM of assembled octahedra (**b**) and tetrahedra (**c**) with averages of particles oriented at their respective symmetry axes (*inset*) (Figure adapted from King et al. 2012 with permission, © American Academy for the Advancement of Science)

ously translated 1 Å radially from the center of symmetry, until no two adjacent trimers had any close contacts. Next, each trimeric protein in the symmetrical assembly was simultaneously rotated 0.5° about its symmetry axis and the analysis repeated. This was performed 240 times to sample the entire set of rotational conformations. The 20 trimers that could be symmetrically docked into conformations with the most compact protein cages, i.e. the largest number of close contacts but without any steric clashes, were selected for interface redesign, and Rosetta was then used to design favorable interactions at the trimer-trimer interface.

35 *de novo* protein-protein interfaces were designed from these 20 proteins with an average of 9 mutations per design, of which 24 expressed as soluble proteins and 3 oligomerized into robust, symmetrical assemblies – one octahedral and two

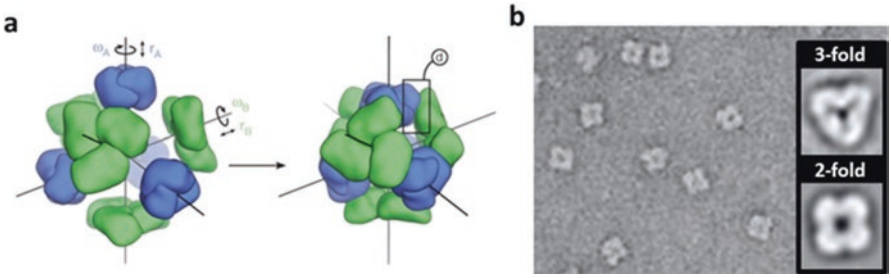

Fig. 8.16 Design of a tetrahedral heteroprotein cage. (**a**) Design strategy. Two oligomeric proteins were arranged at their respective symmetry axes for interface design, for details see the text. (**b**) TEM of assembled particles. *Inset* is averages of particles oriented at their respective axes (Adapted with permission from King et al. 2014, © Macmillan Publishing Ltd)

tetrahedral. Although the success rate of this approach was low, the crystal structures of those proteins that successfully assembled found that they were in close agreement with computational models, representing an impressive achievement.

This approach was further extended to design protein cages in which a trimeric protein was docked at the faces of a tetrahedron and either a dimeric or a trimeric protein was docked at the edges or vertices respectively (Fig. 8.16) (King et al. 2014). The rotational and translational space of both proteins was sampled simultaneously, resulting in a hetero-protein interface that was designed and optimized. In this case, 57 different designed hetero-protein pairs were expressed and characterized experimentally. Of these, four designs were characterized crystallographically. These four tetrahedral protein cages, three with a trimer-trimer symmetry pair and one with a trimer-dimer symmetry pair, were also found to overlay very closely with their computationally designed structures.

The examples above illustrate both the advantages and disadvantages associated with flexible and rigid approaches to assembling proteins. Our laboratory has recently focused on using higher-order symmetry elements to design protein assemblies represented by tetramer-trimer (Sciore et al. 2016), and trimer-trimer (Sciore et al., manuscript in preparation) symmetry pairs. In particular, avoiding the dimeric symmetry elements used in most of the studies discussed above greatly restricts the potential number of geometries that a protein cage can form without explicitly needing to design in a particular dihedral angle connecting the two symmetry elements. In these studies, we first selected a trimeric protein building block with its C-terminus located near the 'vertices' of the triangle formed from the three subunits. To assemble this building block into either octahedral or tetrahedral protein cages we attached at the C-terminus either tetrameric or trimeric *de novo* designed coiled-coils. We then used a modified version of the sampling algorithm developed by King et al. (2012, 2014) discussed above to determine the approximate minimum length of a flexible linker needed to connect the C-terminus of the trimeric building block pro-

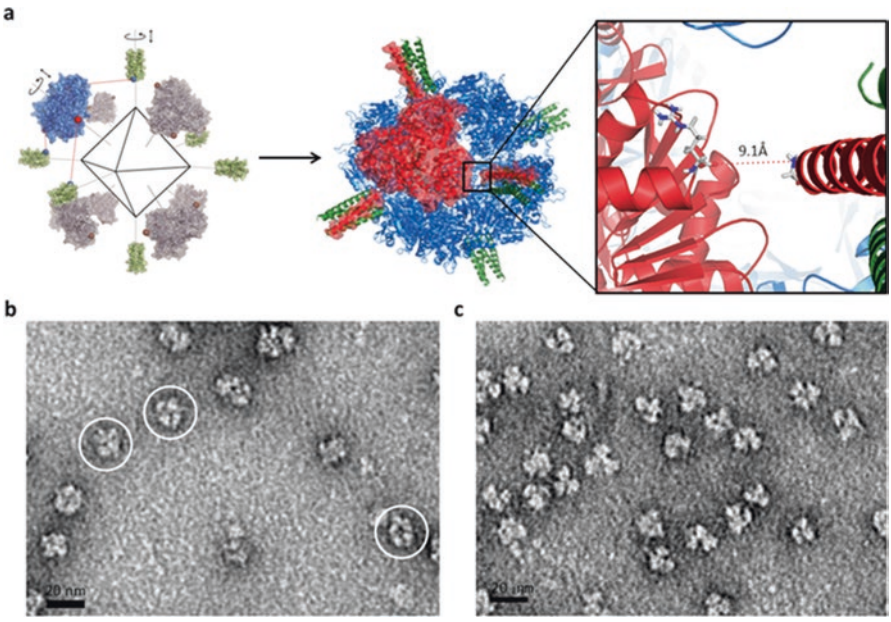

Fig. 8.17 Design of a flexibly-linked protein cage. (**a**) Design strategy: the two oligomeric proteins were aligned on their symmetry axes and the structure with the shortest inter-terminus distance was measured, for details see the text. This value was used to design the flexible linker length. (**b**, **c**) TEM images of the assembled octahedra (**b**) and tetrahedra (**c**)

tein with the N-terminus of the coiled-coils. The modeling indicated that the closest approach between the two design elements without unfavorable steric clashes was about 9 Å for the octahedron and 6 Å for the tetrahedron, which could in principle be bridged by a minimum of two to three residues.

From these computational models, we designed fusion proteins with trimer-trimer and trimer-tetramer symmetry pairs and a glycine-rich linker that varied between 2 and 8 residues in length (Fig. 8.17). In practice, a 4-residue linker proved optimal for the construction of an octahedral protein cage from a trimer-tetramer symmetry pair, whereas an 8-residue linker was required to form a tetrahedron from a trimer-trimer symmetry pair. Fusion proteins with fewer residues in the linker all assembled into a broad range of larger, spherical species. These studies demonstrate that cages of well-defined subunit composition and geometry can be constructed in a relatively simple manner that, in principle, should be highly generalizable. Although this "semi-flexible" approach does not produce as precisely defined or as rigid cages as by interface design, it requires neither sophisticated computational resources, nor extensive screening of many constructs to identify designs that assemble correctly.

8.5 Conclusions

The design of new symmetry-assembled protein nanomaterials will continue to present both interesting challenges and opportunities in the coming years. Research in this area continues to accelerate and there are still many potential avenues to be explored. Currently, research efforts have been primarily focused on exploring the principles of symmetry-directed protein assembly and in particular approaches to correctly orient symmetry elements to achieve the desired protein geometry. These fundamental studies are important, as the utility of assembling proteins into larger structures will only become apparent after methods are developed that allow this to be accomplished in a reliable and routine manner.

In the meantime, there is valuable work to be done investigating whether the current approaches to *de novo* designed protein assemblies can be adapted for, and more significantly, improve upon the range of applications that natural protein assemblies have been used for. For example, the design of protein cages in which enzymatic activity is integrated into the structure promises to be an especially interesting avenue of investigation that could lead to nano-devices that incorporate multiple catalytic activities in a spatially defined manner. Such applications will benefit from an expanded a library of *de novo* designed protein cages. One could imagine that the synthesis of a range of precisely-sized nanoparticles from functionalized protein cages with different interior cavities would be highly attractive for investigations into quantum phenomena.

In summary, the future is bright for symmetrical *de novo* designed protein assemblies. As the design principles described in this chapter, first articulated just fifteen years ago, are refined and perfected, there will be numerous potential applications for these new biological devices in nano-technology and medicine.

References

Abal M, Andreu JM, Barasoain I (2003) Taxanes: microtubule and centrosome targets, and cell cycle dependent mechanisms of action. Curr Cancer Drug Targets 3(3):193–203

Abe S, Hirata K, Ueno T, Morino K, Shimizu N, Yamamoto M, Takata M, Yashima E, Watanabe Y (2009) Polymerization of phenylacetylene by rhodium complexes within a discrete space of apo-ferritin. J Am Chem Soc 131(20):6958–6960. doi:10.1021/ja901234j

Aljabali AAA, Shukla S, Lomonossoff GP, Steinmetz NF, Evans DJ (2013) CPMV-DOX delivers. Mol Pharm 10(1):3–10. doi:10.1021/mp3002057

Allen M, Bulte JWM, Liepold L, Basu G, Zywicke HA, Frank JA, Young M, Douglas T (2005) Paramagnetic viral nanoparticles as potential high-relaxivity magnetic resonance contrast agents. Magn Reson Med 54(4):807–812. doi:10.1002/mrm.20614

André I, Bradley P, Wang C, Baker D (2007) Prediction of the structure of symmetrical protein assemblies. Proc Natl Acad Sci 104(45):17656–17661. doi:10.1073/pnas.0702626104

Ashley CE, Carnes EC, Phillips GK, Durfee PN, Buley MD, Lino CA, Padilla DP, Phillips B, Carter MB, Willman CL, Brinker CJ, Caldeira JC, Chackerian B, Wharton W, Peabody DS (2011) Cell-specific delivery of diverse cargos by bacteriophage MS2 virus-like particles. ACS Nano 5(7):5729–5745. doi:10.1021/nn201397z

Atsushi M, Takio H, Takashi M, Hiroshi Y, Tomoaki H, Yukiharu U, Takashi F, Shigeo Y, Ichiro Y (2006) Floating nanodot gate memory devices based on biomineralized inorganic nanodot array as a storage node. Jpn J Appl Phys 45(1L):L1

Babapoor S, Neef T, Mittelholzer C, Girshick T, Garmendia A, Shang H, Khan MI, Burkhard P (2011) A novel vaccine using nanoparticle platform to present immunogenic m2e against avian influenza infection. Influenza Res Treat 2011:12. doi:10.1155/2011/126794

Banerjee PS, Ostapchuk P, Hearing P, Carrico I (2010) Chemoselective attachment of small molecule effector functionality to human adenoviruses facilitates gene delivery to cancer cells. J Am Chem Soc 132(39):13615–13617. doi:10.1021/ja104547x

Baranova E, Fronzes R, Garcia-Pino A, Van Gerven N, Papapostolou D, Pehau-Arnaudet G, Pardon E, Steyaert J, Howorka S, Remaut H (2012) SbsB structure and lattice reconstruction unveil Ca2+ triggered S-layer assembly. Nature 487(7405):119–122. doi:10.1038/nature11155

Bode SA, Minten IJ, Nolte RJM, Cornelissen JJLM (2011) Reactions inside nanoscale protein cages. Nanoscale 3(6):2376–2389. doi:10.1039/C0NR01013H

Boyle AL, Bromley EHC, Bartlett GJ, Sessions RB, Sharp TH, Williams CL, Curmi PMG, Forde NR, Linke H, Woolfson DN (2012) Squaring the circle in peptide assembly: from fibers to discrete nanostructures by de Novo design. J Am Chem Soc 134(37):15457–15467. doi:10.1021/ja3053943

Brodin JD, Ambroggio XI, Tang C, Parent KN, Baker TS, Tezcan FA (2012) Metal-directed, chemically tunable assembly of one-, two- and three-dimensional crystalline protein arrays. Nat Chem 4(5):375–382

Brumfield S, Willits D, Tang L, Johnson JE, Douglas T, Young M (2004) Heterologous expression of the modified coat protein of Cowpea chlorotic mottle bromovirus results in the assembly of protein cages with altered architectures and function. J Gen Virol 85(Pt 4):1049–1053. doi:10.1099/vir.0.19688-0

Comellas-Aragones M, Engelkamp H, Claessen VI, Sommerdijk NAJM, Rowan AE, Christianen PCM, Maan JC, Verduin BJM, Cornelissen JJLM, Nolte RJM (2007) A virus-based single-enzyme nanoreactor. Nat Nano 2(10):635–639. doi:10.1038/nnano.2007.299

Cormode DP, Jarzyna PA, Mulder WJM, Fayad ZA (2010) Modified natural nanoparticles as contrast agents for medical imaging. Adv Drug Deliv Rev 62(3):329–338. doi:10.1016/j.addr.2009.11.005

Das R, André I, Shen Y, Wu Y, Lemak A, Bansal S, Arrowsmith CH, Szyperski T, Baker D (2009) Simultaneous prediction of protein folding and docking at high resolution. Proc Natl Acad Sci U S A 106(45):18978–18983. doi:10.1073/pnas.0904407106

Dominguez R, Holmes KC (2011) Actin structure and function. Annu Rev Biophys 40:169–186. doi:10.1146/annurev-biophys-042910-155359

Donaldson B, Al-Barwani F, Young V, Scullion S, Ward V, Young S (2015) Virus-like particles, a versatile subunit vaccine platform. In: Foged C, Rades T, Perrie Y, Hook S (eds) Subunit vaccine delivery. Advances in delivery science and technology. Springer, New York, pp 159–180. doi:10.1007/978-1-4939-1417-3_9

Dong H, Paramonov SE, Hartgerink JD (2008) Self-assembly of alpha-helical coiled coil nanofibers. J Am Chem Soc 130(41):13691–13695. doi:10.1021/ja8037323

El Bissati K, Zhou Y, Dasgupta D, Cobb D, Dubey JP, Burkhard P, Lanar DE, McLeod R (2014) Effectiveness of a novel immunogenic nanoparticle platform for Toxoplasma peptide vaccine in HLA transgenic mice. Vaccine 32(26):3243–3248. doi:10.1016/j.vaccine.2014.03.092

Engelhardt H, Peters J (1998) Structural research on surface layers: a focus on stability, surface layer homology domains, and surface layer–cell wall interactions. J Struct Biol 124(2–3):276–302. doi:10.1006/jsbi.1998.4070

Flenniken ML, Liepold LO, Crowley BE, Willits DA, Young MJ, Douglas T (2005) Selective attachment and release of a chemotherapeutic agent from the interior of a protein cage architecture. Chem Commun (Camb) 28(4):447–449. doi:10.1039/b413435d

Flenniken ML, Uchida M, Liepold LO, Kang S, Young MJ, Douglas T (2009) A library of protein cage architectures as nanomaterials. Curr Top Microbiol Immunol 327:71–93

Fletcher JM, Harniman RL, Barnes FRH, Boyle AL, Collins A, Mantell J, Sharp TH, Antognozzi M, Booth PJ, Linden N, Miles MJ, Sessions RB, Verkade P, Woolfson DN (2013) Self-assembling cages from coiled-coil peptide modules. Science 340(6132):595–599. doi:10.1126/science.1233936

Flexman JA, Cross DJ, Lewellen BL, Miyoshi S, Kim Y, Minoshima S (2008) Magnetically targeted viral envelopes: a PET investigation of initial biodistribution. IEEE Trans NanoBiosci 7(3):223–232. doi:10.1109/tnb.2008.2002288

Garcia JA (2011) Sipuleucel-T in patients with metastatic castration-resistant prostate cancer: an insightforoncologists.TherapeutAdvMedOncol3(2):101–108.doi:10.1177/1758834010397692

Ghadiri MR, Granja JR, Milligan RA, McRee DE, Khazanovich N (1993) Self-assembling organic nanotubes based on a cyclic peptide architecture. Nature 366(6453):324–327. doi:10.1038/366324a0

Ghosh D, Lee Y, Thomas S, Kohli AG, Yun DS, Belcher AM, Kelly KA (2012) M13-templated magnetic nanoparticles for targeted in vivo imaging of prostate cancer. Nat Nanotechnol 7(10):677–682. doi:10.1038/nnano.2012.146

Haines-Butterick L, Rajagopal K, Branco M, Salick D, Rughani R, Pilarz M, Lamm MS, Pochan DJ, Schneider JP (2007) Controlling hydrogelation kinetics by peptide design for three-dimensional encapsulation and injectable delivery of cells. Proc Natl Acad Sci 104(19):7791–7796. doi:10.1073/pnas.0701980104

Hooker JM, O'Neil JP, Romanini DW, Taylor SE, Francis MB (2008) Genome-free viral capsids as carriers for positron emission tomography radiolabels. Mol Imaging Biol: MIB: Off Publ Acad of Mol Imaging 10(4):182–191. doi:10.1007/s11307-008-0136-5

Huang P-S, Love JJ, Mayo SL (2007) A de novo designed protein–protein interface. Protein Sci 16(12):2770–2774. doi:10.1110/ps.073125207

Huang RK, Steinmetz NF, Fu C-Y, Manchester M, Johnson JE (2011) Transferrin-mediated targeting of bacteriophage HK97 nanoparticles into tumor cells. Nanomedicine (London, England) 6(1):55–68. doi:10.2217/nnm.10.99

Ilk N, Kupcu S, Moncayo G, Klimt S, Ecker RC, Hofer-Warbinek R, Egelseer EM, Sleytr UB, Sara M (2004) A functional chimaeric S-layer-enhanced green fluorescent protein to follow the uptake of S-layer-coated liposomes into eukaryotic cells. Biochem J 379(Pt 2):441–448. doi:10.1042/BJ20031900

Ilk N, Egelseer EM, Sleytr UB (2011) S-layer fusion proteins – construction principles and applications. Curr Opin Biotechnol 22(6):824–831. doi:10.1016/j.copbio.2011.05.510

Indelicato G, Wahome N, Ringler P, Müller Shirley A, Nieh M-P, Burkhard P, Twarock R (2016) Principles governing the self-assembly of coiled-coil protein nanoparticles. Biophys J 110(3):646–660. doi:dx.doi.org/10.1016/j.bpj.2015.10.057

Ishii D, Kinbara K, Ishida Y, Ishii N, Okochi M, Yohda M, Aida T (2003) Chaperonin-mediated stabilization and ATP-triggered release of semiconductor nanoparticles. Nature 423(6940):628–632

Jennings GT, Bachmann MF (2009) Immunodrugs: therapeutic VLP-based vaccines for chronic diseases. Annu Rev Pharmacol Toxicol 49(1):303–326. doi:10.1146/annurev-pharmtox-061008-103129

Jha RK, Leaver-Fay A, Yin S, Wu Y, Butterfoss GL, Szyperski T, Dokholyan NV, Kuhlman B (2010) Computational design of a PAK1 binding protein. J Mol Biol 400(2):257–270. doi:10.1016/j.jmb.2010.05.006

Jutz G, van Rijn P, Miranda BS, Boeker A (2015) Ferritin: a versatile building block for bionanotechnology. Chem Rev 115(4):1653–1701. doi:10.1021/cr400011b

Kaba SA, Brando C, Guo Q, Mittelholzer C, Raman S, Tropel D, Aebi U, Burkhard P, Lanar DE (2009) A nonadjuvanted polypeptide nanoparticle vaccine confers long-lasting protection against rodent malaria. J Immunol 183(11):7268–7277. doi:10.4049/jimmunol.0901957

Kaiser CR, Flenniken ML, Gillitzer E, Harmsen AL, Harmsen AG, Jutila MA, Douglas T, Young MJ (2007) Biodistribution studies of protein cage nanoparticles demonstrate broad tissue distribution and rapid clearance *in vivo*. Int J Nanomedicine 2(4):715–733

Kawano M, Matsui M, Handa H (2013) SV40 virus-like particles as an effective delivery system and its application to a vaccine carrier. Expert Rev Vaccines 12(2):199–210. doi:10.1586/erv.12.149

Kazunori I, Yukiharu U, Prakaipetch P, Hiroshi Y, Tomoaki H, Takashi F, Ichiro Y (2007) Low-temperature polycrystalline silicon thin film transistor flash memory with ferritin. Jpn J Appl Phys 46(9L):L804

Kimchi-Sarfaty C, Arora M, Sandalon Z, Oppenheim A, Gottesman MM (2003) High cloning capacity of in vitro packaged SV40 vectors with No SV40 virus sequences. Hum Gene Ther 14(2):167–177. doi:10.1089/104303403321070865

Kimchi-Sarfaty C, Vieira WD, Dodds D, Sherman A, Kreitman RJ, Shinar S, Gottesman MM (2006) SV40 Pseudovirion gene delivery of a toxin to treat human adenocarcinomas in mice. Cancer Gene Ther 13(7):648–657

King N, Sheffler W, Sawaya M, Vollmar B, Sumida J, Andre I, Gonen T, Yeates T, Baker D (2012) Computational design of self-assembling protein nanomaterials with atomic level accuracy. Science 6085(336):1171–1174

King NP, Bale JB, Sheffler W, McNamara DE, Gonen S, Gonen T, Yeates TO, Baker D (2014) Accurate design of co-assembling multi-component protein nanomaterials. Nature 510(7503):103–107. doi:10.1038/nature13404

Kiyohito Y, Shigeo Y, Shinya K, Atsushi M, Yukiharu U, Takashi F, Ichiro Y (2007) Effects of dot density and dot size on charge injection characteristics in nanodot array produced by protein supramolecules. Jpn J Appl Phys 46(11R):7549

Klem MT, Willits D, Solis DJ, Belcher AM, Young M, Douglas T (2005) Bio-inspired synthesis of protein-encapsulated CoPt nanoparticles. Adv Funct Mater 15(9):1489–1494. doi:10.1002/adfm.200400453

Kobayashi N, Yanase K, Sato T, Unzai S, Hecht MH, Arai R (2015) Self-assembling nano-architectures created from a protein nano-building block using an intermolecularly folded dimeric de Novo protein. J Am Chem Soc 137(35):11285–11293. doi:10.1021/jacs.5b03593

Kramer RM, Sowards LA, Pender MJ, Stone MO, Naik RR (2005) Constrained iron catalysts for single-walled carbon nanotube growth. Langmuir 21(18):8466–8470. doi:10.1021/la0506729

Lai Y-T, Cascio D, Yeates TO (2012) Structure of a 16-nm cage designed by using protein oligomers. Science 336(6085):1129–1129

Lai Y-T, Reading E, Hura GL, Tsai K-L, Laganowsky A, Asturias FJ, Tainer JA, Robinson CV, Yeates TO (2014) Structure of a designed protein cage that self-assembles into a highly porous cube. Nat Chem 6(12):1065–1071. doi:10.1038/nchem.2107

Lanci CJ, MacDermaid CM, S-g K, Acharya R, North B, Yang X, Qiu XJ, DeGrado WF, Saven JG (2012) Computational design of a protein crystal. Proc Natl Acad Sci U S A 109(19):7304–7309. doi:10.1073/pnas.1112595109

Landry SJ, Gierasch LM (1991) The chaperonin GroEL binds a polypeptide in an alpha-helical conformation. Biochemistry 30(30):7359–7362

Lockney DM, Guenther RN, Loo L, Overton W, Antonelli R, Clark J, Hu M, Luft C, Lommel SA, Franzen S (2011) The red clover necrotic mosaic virus capsid as a multifunctional cell targeting plant viral nanoparticle. Bioconjug Chem 22(1):67–73. doi:10.1021/bc100361z

Matthaei JF, DiMaio F, Richards JJ, Pozzo LD, Baker D, Baneyx F (2015) Designing two-dimensional protein arrays through fusion of multimers and interface mutations. Nano Lett 15(8):5235–5239. doi:10.1021/acs.nanolett.5b01499

Maurer P, Jennings GT, Willers J, Rohner F, Lindman Y, Roubicek K, Renner WA, Muller P, Bachmann MF (2005) A therapeutic vaccine for nicotine dependence: preclinical efficacy, and Phase I safety and immunogenicity. Eur J Immunol 35(7):2031–2040. doi:10.1002/eji.200526285

McMillan RA, Howard J, Zaluzec NJ, Kagawa HK, Mogul R, Li Y-F, Paavola CD, Trent JD (2005) A self-assembling protein template for constrained synthesis and patterning of nanoparticle arrays. J Am Chem Soc 127(9):2800–2801. doi:10.1021/ja043827s

Mertig M, Kirsch R, Pompe W, Engelhardt H (1999) Fabrication of highly oriented nanocluster arrays by biomolecular templating. Eur Phys J D-Atomic, Mol Opt Plasma Phys 9(1):45–48

Minten IJ, Claessen VI, Blank K, Rowan AE, Nolte RJM, Cornelissen JJLM (2011) Catalytic capsids: the art of confinement. Chem Sci 2(2):358–362. doi:10.1039/C0SC00407C

Oda T, Iwasa M, Aihara T, Maeda Y, Narita A (2009) The nature of the globular- to fibrous-actin transition. Nature 457(7228):441–445

Padilla JE, Colovos C, Yeates TO (2001) Nanohedra: using symmetry to design self assembling protein cages, layers, crystals, and filaments. Proc Natl Acad Sci U S A 98(5):2217–2221

Patterson DP, Desai AM, Holl MMB, Marsh ENG (2011) Evaluation of a symmetry-based strategy for assembling protein complexes. RSC Adv 1(6):1004–1012. doi:10.1039/c1ra00282a

Patterson DP, Schwarz B, Waters RS, Gedeon T, Douglas T (2014a) Encapsulation of an enzyme cascade within the bacteriophage P22 virus-like particle. ACS Chem Biol 9(2):359–365. doi:10.1021/cb4006529

Patterson DP, Su M, Franzmann TM, Sciore A, Skiniotis G, Marsh ENG (2014b) Characterization of a highly flexible self-assembling protein system designed to form nanocages. Protein Sci 23(2):190–199. doi:10.1002/pro.2405

Picher MM, Kupcu S, Huang C-J, Dostalek J, Pum D, Sleytr UB, Ertl P (2013) Nanobiotechnology advanced antifouling surfaces for the continuous electrochemical monitoring of glucose in whole blood using a lab-on-a-chip. Lab Chip 13(9):1780–1789. doi:10.1039/C3LC41308J

Pleschberger M, Saerens D, Weigert S, Sleytr UB, Muyldermans S, Sára M, Egelseer EM (2004) An S-Layer heavy chain camel antibody fusion protein for generation of a nanopatterned sensing layer to detect the prostate-specific antigen by surface plasmon resonance technology. Bioconjug Chem 15(3):664–671. doi:10.1021/bc049964w

Poobalane S, Thompson KD, Ardó L, Verjan N, Han H-J, Jeney G, Hirono I, Aoki T, Adams A (2010) Production and efficacy of an Aeromonas hydrophila recombinant S-layer protein vaccine for fish. Vaccine 28(20):3540–3547. doi:10.1016/j.vaccine.2010.03.011

Price GD, Badger MR (1989) Expression of human carbonic anhydrase in the cyanobacterium synechococcus PCC7942 creates a high CO(2)-requiring phenotype: evidence for a central role for carboxysomes in the CO(2) concentrating mechanism. Plant Physiol 91(2):505–513

Rajagopal K, Lamm MS, Haines-Butterick LA, Pochan DJ, Schneider JP (2009) Tuning the pH responsiveness of β-Hairpin peptide folding, self-assembly, and hydrogel material formation. Biomacromolecules 10(9):2619–2625. doi:10.1021/bm900544e

Raman S, Machaidze G, Lustig A, Aebi U, Burkhard P (2006) Structure-based design of peptides that self-assemble into regular polyhedral nanoparticles. Nanomedicine 2(2):95–102. doi:10.1016/j.nano.2006.04.007

Raza K, Katare OP, Setia A, Bhatia A, Singh B (2013) Improved therapeutic performance of dithranol against psoriasis employing systematically optimized nanoemulsomes. J Microencapsul 30(3):225–236. doi:10.3109/02652048.2012.717115

Rebeaud F, Bachmann M (2012) Virus-like particles as efficient delivery platform to induce a potent immune response. In: Baschieri S (ed) Innovation in vaccinology. Springer, Dordrecht, pp 87–122. doi:10.1007/978-94-007-4543-8_5

Ringler P, Schulz GE (2003) Self-assembly of proteins into designed networks. Science 302(5642):106–109

Ross PD, Conway JF, Cheng N, Dierkes L, Firek BA, Hendrix RW, Steven AC, Duda RL (2006) A free energy cascade with locks drives assembly and maturation of bacteriophage HK97 capsid. J Mol Biol 364(3):512–525. doi:10.1016/j.jmb.2006.08.048

Rothbauer M, Küpcü S, Sticker D, Sleytr UB, Ertl P (2013) Exploitation of S-layer anisotropy: pH-dependent nanolayer orientation for cellular micropatterning. ACS Nano 7(9):8020–8030

Rothbauer M, Ertl P, Theiler BA, Schlager M, Sleytr UB, Küpcü S (2015) Anisotropic crystalline protein nanolayers as multi-functional biointerface for patterned co-cultures of adherent and non-adherent cells in microfluidic devices. Adv Mater Interfaces 2(1):n/a–n/a. doi:10.1002/admi.201400309

Salick DA, Kretsinger JK, Pochan DJ, Schneider JP (2007) Inherent antibacterial activity of a peptide-based beta-hairpin hydrogel. J Am Chem Soc 129(47):14793–14799. doi:10.1021/ja076300z

Sára M, Sleytr UB (2000) S-Layer proteins. J Bacteriol 182(4):859–868. doi:10.1128/jb.182.4.859-868.2000

Sara M, Pum D, Kupcu S, Messner P, Sleytr UB (1994) Isolation of two physiologically induced variant strains of Bacillus stearothermophilus NRS 2004/3a and characterization of their S-layer lattices. J Bacteriol 176(3):848–860

Sciore A, Su M, Koldewey P, Eschweiler J, Diffley K, Linhares B, Ruotolo B, Bardwell J, Skiniotis G, Marsh ENG (2016) Flexible, symmetry-directed approach to assembling protein cages. Proc Natl Acad Sci U S A 113(31):8681–8686

Shenton W, Pum D, Sleytr UB, Mann S (1997) Synthesis of cadmium sulphide superlattices using self-assembled bacterial S-layers. Nature 389(6651):585–587

Sinclair JC, Davies KM, Venien-Bryan C, Noble MEM (2011) Generation of protein lattices by fusing proteins with matching rotational symmetry. Nat Nano 6(9):558–562. doi:10.1038/nnano.2011.122

Singh S, Zlotnick A (2003) Observed hysteresis of virus capsid disassembly is implicit in kinetic models of assembly. J Biol Chem 278(20):18249–18255. doi:10.1074/jbc.M211408200

Sleytr UB, Beveridge TJ (1999) Bacterial S-layers. Trends Microbiol 7(6):253–260. doi:10.1016/S0966-842X(99)01513-9

Speiser DE, Schwarz K, Baumgaertner P, Manolova V, Devevre E, Sterry W, Walden P, Zippelius A, Conzett KB, Senti G, Voelter V, Cerottini JP, Guggisberg D, Willers J, Geldhof C, Romero P, Kundig T, Knuth A, Dummer R, Trefzer U, Bachmann MF (2010) Memory and effector CD8 T-cell responses after nanoparticle vaccination of melanoma patients. J Immunother (Hagerstown, Md: 1997) 33(8):848–858. doi:10.1097/CJI.0b013e3181f1d614

Spohn G, Keller I, Beck M, Grest P, Jennings GT, Bachmann MF (2008) Active immunization with IL-1 displayed on virus-like particles protects from autoimmune arthritis. Eur J Immunol 38(3):877–887. doi:10.1002/eji.200737989

Stephanopoulos N, Tong GJ, Hsiao SC, Francis MB (2010) Dual-surface modified virus capsids for targeted delivery of photodynamic agents to cancer cells. ACS Nano 4(10):6014–6020. doi:10.1021/nn1014769

Štokrová J, Palková Z, Fischer L, Richterová Z, Korb J, Griffin BE, Forstová J (1999) Interactions of heterologous DNA with polyomavirus major structural protein, VP1. FEBS Lett 445(1):119–125. doi:10.1016/S0014-5793(99)00003-4

Stranges PB, Machius M, Miley MJ, Tripathy A, Kuhlman B (2011) Computational design of a symmetric homodimer using β-strand assembly. Proc Natl Acad Sci 108(51):20562–20567. doi:10.1073/pnas.1115124108

Takuro M, Nozomu M, Kenji I, Ken-Ichi S, Kiyotaka S, Ichiro Y (2007) Direct production of a two-dimensional ordered array of ferritin-nanoparticles on a silicon substrate. Jpn J Appl Phys 46(7L):L713

Teunissen EA, de Raad M, Mastrobattista E (2013) Production and biomedical applications of virus-like particles derived from polyomaviruses. J Control Release 172(1):305–321. doi:10.1016/j.jconrel.2013.08.026

Theil EC (1987) Ferritin: structure, gene regulation, and cellular function in animals, plants, and microorganisms. Annu Rev Biochem 56(1):289–315. doi:10.1146/annurev.bi.56.070187.001445

Uchida M, Terashima M, Cunningham CH, Suzuki Y, Willits DA, Willis AF, Yang PC, Tsao PS, McConnell MV, Young MJ, Douglas T (2008) A human ferritin iron oxide nano-composite magnetic resonance contrast agent. Magn Reson Med 60(5):1073–1081. doi:10.1002/mrm.21761

Ucisik MH, Sleytr UB, Schuster B (2015) Emulsomes meet S-layer proteins: an emerging targeted drug delivery system. Curr Pharm Biotechnol 16(4):392–405. doi:10.2174/1389201016041502181126 56

Ueno T, Suzuki M, Goto T, Matsumoto T, Nagayama K, Watanabe Y (2004) Size-selective olefin hydrogenation by a Pd nanocluster provided in an apo-ferritin cage. Angew Chem Int Ed 43(19):2527–2530. doi:10.1002/anie.200353436

Vabulas RM, Raychaudhuri S, Hayer-Hartl M, Hartl FU (2010) Protein folding in the cytoplasm and the heat shock response. Cold Spring Harb Perspect Biol 2(12). doi:10.1101/cshperspect.a004390

Villard V, Kalyuzhniy O, Riccio O, Potekhin S, Melnik TN, Kajava AV, Ruegg C, Corradin G (2006) Synthetic RGD-containing alpha-helical coiled coil peptides promote integrin-dependent cell adhesion. J Pept Sci 12(3):206–212. doi:10.1002/psc.707

Wahome N, Pfeiffer T, Ambiel I, Yang Y, Keppler OT, Bosch V, Burkhard P (2012) Conformation-specific display of 4E10 and 2F5 epitopes on self-assembling protein nanoparticles as a potential HIV vaccine. Chem Biol Drug Des 80(3):349–357. doi:10.1111/j.1747-0285.2012.01423.x

Weigert S, Sára M (1996) Ultrafiltration membranes prepared from crystalline bacterial cell surface layers as model systems for studying the influence of surface properties on protein adsorption. J Membr Sci 121(2):185–196. doi:10.1016/S0376-7388(96)00176-7

Wiessner C, Wiederhold KH, Tissot AC, Frey P, Danner S, Jacobson LH, Jennings GT, Luond R, Ortmann R, Reichwald J, Zurini M, Mir A, Bachmann MF, Staufenbiel M (2011) The second-generation active Abeta immunotherapy CAD106 reduces amyloid accumulation in APP transgenic mice while minimizing potential side effects. J Neurosci 31(25):9323–9331. doi:10.1523/jneurosci.0293-11.2011

Woolfson DN (2010) Building fibrous biomaterials from α-helical and collagen-like coiled-coil peptides. Pept Sci 94(1):118–127. doi:10.1002/bip.21345

Yang Y, Ringler P, Müller SA, Burkhard P (2012) Optimizing the refolding conditions of self-assembling polypeptide nanoparticles that serve as repetitive antigen display systems. J Struct Biol 177(1):168–176. doi:10.1016/j.jsb.2011.11.011

Yang R, Chen L, Yang S, Lv C, Leng X, Zhao G (2014) 2D square arrays of protein nanocages through channel-directed electrostatic interactions with poly([small alpha], l-lysine). Chem Commun 50(22):2879–2882. doi:10.1039/C3CC49306G

Yeates TO, Padilla JE (2002) Designing supramolecular protein assemblies. Curr Opin Struct Biol 12(4):464–470

Yeates TO, Kerfeld CA, Heinhorst S, Cannon GC, Shively JM (2008) Protein-based organelles in bacteria: carboxysomes and related microcompartments. Nat Rev Microbiol 6(9):681–691

Yeates TO, Thompson MC, Bobik TA (2011) The protein shells of bacterial microcompartment organelles. Curr Opin Struct Biol 21(2):223–231. doi:10.1016/j.sbi.2011.01.006

Zhang S, Holmes T, Lockshin C, Rich A (1993) Spontaneous assembly of a self-complementary oligopeptide to form a stable macroscopic membrane. Proc Natl Acad Sci 90(8):3334–3338. doi:10.1073/pnas.90.8.3334

Zhao Q, Chen W, Chen Y, Zhang L, Zhang J, Zhang Z (2011) Self-assembled virus-like particles from rotavirus structural protein VP6 for targeted drug delivery. Bioconjug Chem 22(3):346–352. doi:10.1021/bc1002532